Shock Response of Full Density Nanopolycrystalline Diamond

Kento Katagiri,[1,2,*] Norimasa Ozaki,[1,2] Yuhei Umeda,[1,3] Tetsuo Irifune,[4,5] Nobuki Kamimura,[1] Kohei Miyanishi,[6] Takayoshi Sano,[2] Toshimori Sekine,[1,7] and Ryosuke Kodama[1,2]

[1]*Graduate School of Engineering, Osaka University, Osaka 565-0871, Japan*
[2]*Institute of Laser Engineering, Osaka University, Osaka 565-0871, Japan*
[3]*Institute for Planetary Materials, Okayama University, Tottori 682-0193, Japan*
[4]*Geodynamics Research Center, Ehime University, Ehime 790-0826, Japan*
[5]*Earth-Life Science Institute, Tokyo Institute of Technology, Tokyo 145-0061, Japan*
[6]*RIKEN SPring-8 Center, Hyogo 679-5148, Japan*
[7]*Center for High-Pressure Science and Technology Advanced Research, Shanghai 201203, China*

(Received 26 May 2020; accepted 24 September 2020; published 28 October 2020)

Hugoniot of full-dense nanopolycrystalline diamond (NPD) was investigated up to 1600 GPa. The Hugoniot elastic limit of NPD is 208 (±14) GPa, which is more than twice as high as that of single-crystal diamond. The Hugoniot of NPD is stiffer than that of single-crystal diamond up to 500 GPa, while no significant difference is observed at higher pressures where the elastic precursor is overdriven by a following plastic wave. These findings confirm that the grain boundary strengthening effect recognized in static compression experiments is also effective against high strain-rate dynamic compressions.

DOI: 10.1103/PhysRevLett.125.185701

According to the Hall-Petch relationship [1,2], the hardness of a material increases as its grain size decreases. This effect is known as grain boundary strengthening and is recognized in a variety of materials at ambient conditions [3,4]. Since diamond is the hardest material in nature, the grain boundary strengthening effect in nanopolycrystalline diamond (NPD) [5] has been one of the major interests in the field of materials science. While the high hardness of NPD has been tested in static experiments [3,6], its hardness under high strain-rate dynamic compression is not yet known.

Hugoniot elastic limit (HEL) is defined as the longitudinal pressure (stress) at which a solid undergoes a transition from reversible elastic deformation to irreversible plastic deformation upon dynamic compression [7]. Only a little is known about how the grain size affects the HEL and Hugoniot of polycrystalline materials [8–10], mainly due to the difficulties of synthesizing homogeneous and full-dense polycrystalline samples with different grain sizes. The NPD samples used in this study were full dense and transparent [5], and had an average grain size of 10–20 nm. The grain boundary strengthening effect is known to be strongest at these grain sizes. Since NPD is harder than single-crystal diamond at ambient conditions [3,6] due to the effect of grain boundary strengthening, the HEL of NPD is possibly higher than that of single-crystal diamond. The main issue we address by measuring the HEL of NPD is whether the grain boundary strengthening effect is valid for diamond under high strain rate ($\sim 10^9$ s^{-1}) shock compression. We also measured the Hugoniot of NPD at higher pressures up to 1600 GPa, as it is important for the development of the inertial confinement fusion targets which use nanocrystalline diamond as its ablator material [11].

The experiments were performed at the GEKKO XII laser facility at the Institute of Laser Engineering, Osaka University [12]. The wavelength of the twelve drive lasers in GEKKO XII was 527 or 351 nm, which is the second or the third harmonic wavelength of the neodymium glass laser with a fundamental wavelength of 1054 nm. The focal spot was smoothed using kinoform phase plates. The spot diameters on the target were 1000 and 600 μm for the second and third harmonic wavelengths, respectively. The duration of the laser pulse was 2.5 ns in the full width at half maximum with around 100 ps each for the rise and fall times. To determine the shock-compressed state of the sample, velocity profiles were recorded by a line-imaging velocity interferometer system for any reflector (VISAR) [13] operated with a 532 nm probe light. The velocity sensitivities of VISARs were 7.523 and 4.476 km/s/fringe. The VISAR system had a spatial resolution of $\sim$6 μm and a temporal resolution of $\sim$50 ps. The experimental uncertainties of measured velocities were less than 5% of the velocity sensitivities. See Supplemental Material [14] for the summarized shock data and more detail about the evaluation of uncertainties.

The NPD samples were synthesized using a multi-anvil cell at Ehime University. Each sample was polished to a thickness of 70–100 μm and had a density of 3.514 (±0.003) g/cm^3 [18]. The shock target is schematically shown in Fig. 1. In this work, z-cut α-quartz and polystyrene were used as the pressure standards. The

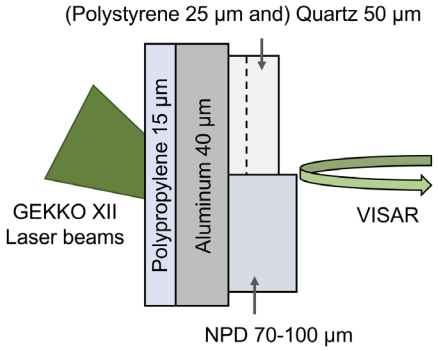

FIG. 1. Experimental configuration of the NPD Hugoniot measurements. For the shots with peak longitudinal pressures in NPD of 936 (±13) GPa or higher, a 50 μm thick z-cut α quartz attached to aluminum was used as a pressure standard. For the other shots [630 (±9) GPa or lower], a 25 μm thick polystyrene sandwiched between aluminum and quartz was used as a pressure standard instead. In both cases, an antireflection coating for 532 nm was on the VISAR irradiation side of the quartz.

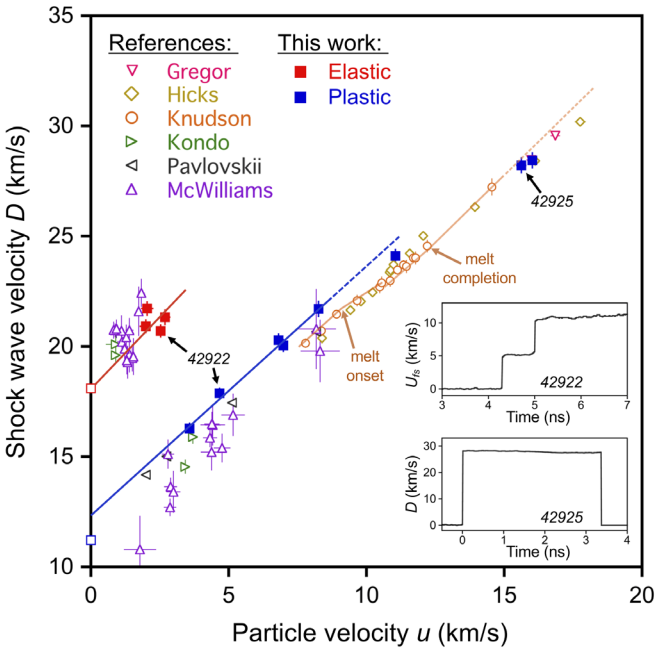

FIG. 2. Shock wave velocity versus particle velocity of NPD. Filled squares represent the elastic state (red) and plastic state (blue) obtained in this work. These data of the elastic state and the plastic state below the expected melt onset ($u < 9$ km/s) are linearly fitted by red and blue solid lines, respectively. Blue dotted line is the extrapolation of the plastic fit. Open squares are the ambient longitudinal sound velocity (red) and the bulk sound velocity (blue) of NPD [18]. Other symbols are reference data of single-crystal diamond [23,25–28] and polycrystalline diamond [24]. The shown plots of Hicks *et al.* (open yellow diamond) [28] are the reanalyzed data [29] using updated quartz Hugoniot [21]. The diamond Hugoniot around its melt boundaries predicted by *ab initio* molecular dynamics simulations [24] (orange solid lines) and its extrapolation (orange dashed line) are also shown. Insets are the typical VISAR profiles showing the free-surface velocity forming a continuous elastic-plastic two-wave structure at the rear surface of the NPD sample (top) and the velocity of the shock wave propagating inside of the NPD sample (bottom). In both profiles, time 0 denotes the time for the shock wave to enter the NPD from the aluminum.

measured thickness of the glue between these materials was less than 1 μm for each target.

The compressed state of NPD was determined by the impedance mismatching method [19] using the known Hugoniots of quartz [20], aluminum [21], and polystyrene [22]. At peak pressures of 496 (±8) GPa or lower in NPD, the free-surface velocities exhibited elastic-plastic two-wave structures and the impedance mismatching method for two-wave structures described by McWilliams *et al.* [23] was used to determine the shocked state. When the applied pressure in NPD is 630 (±9) GPa, however, a single wave structure was observed at the rear surface as the elastic wave was overdriven by the plastic wave. In this case, the average shock wave velocity of NPD was determined by simply dividing the initial sample thickness by the shock wave propagation time. For the shots with a peak pressure of 936 (±13) GPa or higher, NPD was reflective under compression, thus the shock wave velocities were time resolved. The obtained relationship between the shock wave velocity (D) and the particle velocity (u) of NPD below the expected melt onset ($u < 9.1$ km/s [24]) can be linearly fitted by $D_e = (1.297 \pm 0.266)\ u_e + (18.11 \pm 0.01)$ and $D_p = (1.130 \pm 0.062)\ u_p + (12.39 \pm 0.39)$ for the elastic and plastic responses, respectively (Fig. 2). Here, the longitudinal sound velocity of NPD at ambient conditions [18] was used to get the elastic linear fit. The longitudinal pressure P and density ρ of the shocked state can be obtained from the measured shock wave velocity and particle velocity via the Rankin-Hugoniot equations [23]:

$$P_2 = P_1 + \rho_1 (D_2 - u_1)(u_2 - u_1), \tag{1}$$

$$\rho_2 = \rho_1 \frac{D_2 - u_1}{D_2 - u_2}, \tag{2}$$

where subscripts 1 and 2 denote the conditions ahead of and behind the shock front, respectively.

The relationships between the longitudinal pressure in preceding elastic deformation and the peak pressure in subsequent plastic deformation for NPD and single-crystal diamond [23] are shown in Fig. 3. The results show that the longitudinal pressures in elastic precursors vary between 146 (±15) and 202(±13) GPa. Notably, the longitudinal pressure in the preceding elastic deformation in NPD is lower when the peak pressure is higher. However, some other materials are known to exhibit a higher elastic amplitude for a higher peak pressure under shock compression [30]. This is especially controversial for the case of single-crystal diamond. Lang *et al.* observed during their powder gun experiments that the amplitude in the elastic

precursor is higher when the peak pressure is lower [31]. McWilliams *et al.*, however, compressed single-crystal diamonds by laser-driven shocks and found that the amplitude in the elastic precursor is higher when the peak pressure is higher [23]. Both groups observed the same tendency for the three directions of diamond : ⟨100⟩, ⟨110⟩, and ⟨111⟩. Later, Winey *et al.* conducted plate impact experiments and showed that the elastic wave amplitudes for ⟨110⟩ and ⟨111⟩ diamond increase considerably with increasing peak stresses [32]. Winey *et al.* described that the observed difference in trend between their results and Lang's results could be due to the difference in the applied peak stresses. Therefore, the correlation between elastic wave and plastic wave is evident, and it possibly depends on the strain rate and duration of the compression, the amplitude of the applied peak stress, and the grain size of diamond.

In the case of NPD, the dislocation propagation can be prevented at grain boundaries, hence the stress inhomogeneities in elastically compressed nanograins due to differences in orientations and diameters between neighboring nanograins can be sustained up to a certain limit (HEL). When applied peak pressure is high, however, the elastic response would be disturbed by the interference of the plastic wave, which might weaken the grain boundary strengthening effect and reduce the amplitude of the elastic wave. Understanding the correlation between elastic and plastic deformations can improve the modeling of ultrafast deformation [33], including grain boundary strengthening effect and grain refinement process of ultrahard materials under dynamic compression, as the current models often assume that the preceding elastic wave would not be disturbed by the following plastic wave.

Among the elastic-plastic two-wave structures observed in this work, the highest longitudinal pressure of the elastic precursor was 202 (±13) GPa, which was observed when the peak pressure of the following plastic deformation was the lowest (Fig. 3). When the peak pressure is reduced, only a pure elastic wave is formed from a certain point, and this point is the HEL of the shocked material. The linear fit for the NPD data shown in Fig. 3 suggests that the longitudinal pressures in elastic deformation and plastic deformation would become equal at 208 (±14) GPa, suggesting that the HEL of NPD is 208 (±14) GPa. This value is more than twice as high as the HELs of single-crystal diamond measured by using a similar method, which are 80.1 (±12.4), 80.7 (±5.8), and 60.4 (±3.3) GPa for the compression directions along ⟨100⟩ (type Ia), ⟨110⟩ (type Ia and IIa), and ⟨111⟩ (type Ib), respectively [23]. Sokol *et al.* performed dynamic compression experiments on a ceramic ($MgAl_2O_3$) and observed that the HEL of $MgAl_2O_3$ with an initial grain size of 0.14 μm is ∼1.7 times higher than that with 170 μm [8], which is comparable to the difference observed in the HELs of single-crystal diamond and NPD. A similar tendency was

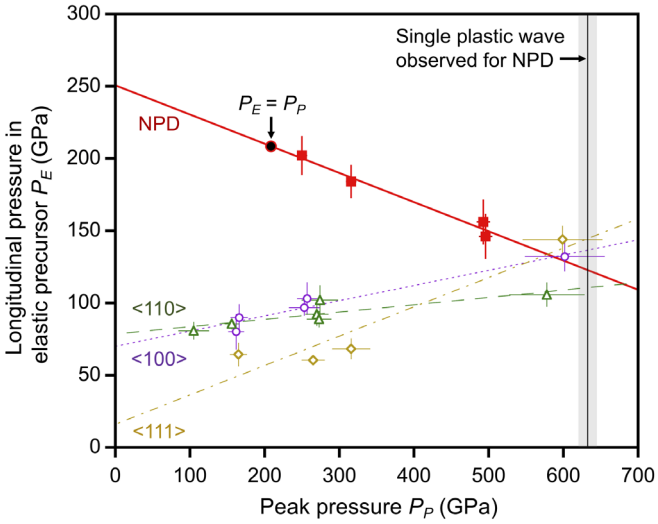

FIG. 3. Longitudinal pressure in preceding elastic deformation versus the corresponding peak pressure of diamond. Red squares show the NPD data obtained in this work. The black circle shows the point where the elastic pressure is equal to the plastic pressure [$P_E = P_P = 208$ (±14) GPa] along the NPD fitting line (red line). The data for laser shock compressed single-crystal diamond with three different orientations ⟨100⟩ (purple circle, dotted line), ⟨110⟩ (green triangle, dashed line), and ⟨111⟩ (yellow diamond, dot-dashed line) are also shown for comparison [23].

observed for dynamically compressed polycrystalline iron with micrometer-sized grains [9]. Since HEL defines the material strength under shock compression, these results show that the effect of grain boundary strengthening recognized at ambient conditions is also effective under high strain-rate shock compression.

The difference in the HEL between NPD and single-crystal diamond obtained in this study was greater than the difference in their Knoop hardness measured under static compression. Sumiya *et al.* reported that the Knoop hardness of NPD at room temperature is about 130 GPa, which is 0%–10% higher than that of type IIa single-crystal diamond and 40%–65% higher than that of type Ib single-crystal diamond [6]. These results suggest that the grain boundary strengthening effect on the resistance to deformation of ultrahard materials such as diamond is strain-rate dependent.

The obtained relationship between longitudinal pressure and density (Fig. 4) shows that the Hugoniot of NPD is stiffer than that of single-crystal diamond [23,25,26] at pressures up to ∼500 GPa. The observed stiffness of plastically deformed NPD can be explained by the high amplitude of the elastic wave as the elastic-plastic two-wave structure is formed at pressures below 500 GPa. At higher pressures where the single (overdriven) plastic wave is observed, the pressure-density relationship of NPD is almost identical to that of single-crystal diamond. The observed relationship between shock wave velocity and particle velocity of NPD (Fig. 2) is also different from that

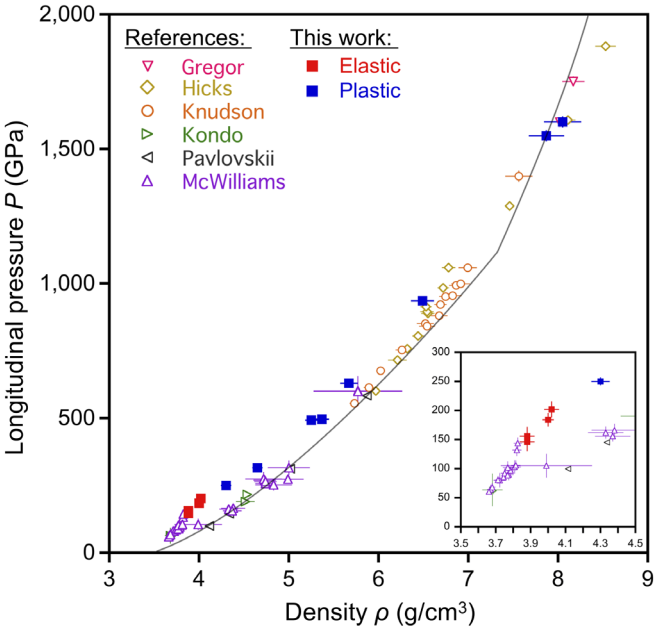

FIG. 4. Longitudinal pressure versus density of shock-compressed NPD. The symbols and coloration are the same as in Fig. 2. The gray curves are the multiphase EOS of diamond calculated by DFT-MD [35]. Inset shows more detail.

of single-crystal diamond, particularly at the low particle velocity region ($u < 7$ km/s) where elastic-plastic two-wave structure is observed [14]. According to the molecular dynamics simulations performed by Bringa *et al.*, the flow stress of nanocrystalline copper under shock loading depends on its grain size [10]. Thus, it is interesting to see how nanograin boundaries in NPD increase its strength against the plastic flow. However, it is difficult to rigorously characterize the plastic state by the presenting experimental method when elastic-plastic two-wave structure is within the sample [32]. Further experiments with different experimental configurations [34] and numerical simulations are needed to rigorously analyze the grain size effects on the strength of plastically deformed diamond, and this would lead to a better understanding of the difference in the observed trends of the elastic pressure with respect to the peak pressure between NPD and single-crystal diamond.

The presence of porosity in the initial sample will increase the shock temperature, resulting in the material on a different Hugoniot, but the observed stiffness in NPD is due to the grain size as the NPD used in the present work had no significant porosity. Gregor *et al.* previously reported the Hugoniot of porous nanocrystalline diamond (~5% less dense than single-crystal diamond) at pressures of 1100–2500 GPa [27]. They found that their nanocrystalline diamond has a stiffer Hugoniot than single-crystal diamond above 1100 GPa, and they described that the observed stiffness can be due to the porosity of the sample. As our results show, the Hugoniot of full-dense NPD is identical to that of single-crystal diamond above the expected melting point, the stiffness of nanocrystalline diamond observed by Gregor *et al.* is only due to its porosity, as they deduced. Our results show that the density change accompanied by melting or a phase transition to a denser solid phase would be small, as also seen in single-crystal diamond [28].

Nanocrystalline diamond is currently considered as the ablator material for inertial confinement fusion (ICF) researches to compress the hydrogen fuel [11] and the highly accurate prediction of shock wave propagation in the ablator material is required for successful ICF implosions. The observed difference in the shock equation of states of NPD and single-crystal diamond below ~500 GPa opens up the opportunity to study the shock response of the nanocrystalline diamond ablator in more detail as the current ICF experiments set the first shock stress in the diamond at around 600 GPa [11].

In conclusion, we performed a series of shock compression experiments on NPD and showed that the HEL of NPD is 208 (±14) GPa, which is the highest HEL of any materials ever measured. We also found that the Hugoniot of NPD is stiffer than that of single-crystal diamond up to ~500 GPa. These results demonstrate that the grain boundary strengthening effect in diamond, as observed in static compression experiments, is also effective under dynamic compressions. This is key to the development of ultrahard materials during and after high strain-rate compression, which could be extended to various applications such as spacecraft shielding, nanoceramics, and inertial confinement fusion targets.

We thank the GEKKO technical staff for their support during these experiments and Toru Shinmei of GRC for synthesis of NPD. We also thank J. Lintz for valuable comments on the manuscript. The experiments were conducted under the joint research of the Institute of Laser Engineering, Osaka University, Japan. This work was supported by grants from MEXT Quantum Leap Flagship Program (MEXT Q-LEAP) Grant No. JPMXS0118067246, Japan Society for the Promotion of Science (JSPS) KAKENHI (Grants No. 19K21866 and No. 16H02246), and Genesis Research Institute, Inc. (Konpon-ken, Toyota). The NPD sample fabrication was conducted under the support of Joint Research Center Premier Research Institute for Ultrahigh-pressure Science (PRIUS), Ehime University, Japan. We also acknowledge partial support by Center for High-Pressure Science and Technology Advanced Research (HPSTAR), China.

*Corresponding author.
kkatagiri@ef.eie.eng.osaka-u.ac.jp

[1] E. O. Hall, Proc. Phys. Soc. London Sect. B **64**, 747 (1951).
[2] N. J. Petch, J. Iron Steel Inst. **173**, 25 (1953).
[3] H. Sumiya and T. Irifune, J. Matter Res. **22**, 2345 (2007).

[4] N. Nishiyama, T. Taniguchi, H. Ohfuji, K. Yoshida, F. Wakai, B. Kim, H. Yoshida, Y. Higo, A. Holzheid, O. Beermann, T. Irifune, Y. Sakka, and K. Funakoshi, Scr. Mater. **69**, 362 (2013).
[5] T. Irifune, A. Kurio, S. Sakamoto, T. Inoue, and H. Sumiya, Nature (London) **421**, 599 (2003).
[6] H. Sumiya and K. Harano, Diam. Relat. Mater. **24**, 44 (2012).
[7] G. I. Kanel, S. V. Razorenov, and V. E. Fortov, *Shock-Wave Phenomena and the Properties of Condensed Matter* (Springer-Verlag, New York, 2004).
[8] M. Sokol, S. Kalabukhov, R. Shneck, E. Zaretsky, and N. Frage, J. Eur. Ceram. Soc. **37**, 3417 (2017).
[9] R. F. Smith, J. H. Eggert, R. E. Rudd, D. C. Swift, C. A. Bolme, and G. W. Collins, J. Appl. Phys. **110**, 123515 (2011).
[10] E. M. Bringa, A. Caro, Y. Wang, M. Victoria, J. M. McNaney, B. A. Remington, R. F. Smith, B. R. Torralva, and H. V. Swygenhoven, Science **309**, 1838 (2005).
[11] J. S. Ross, D. Ho, J. Milovich, T. Döppner, J. McNaney, A. G. MacPhee, A. Hamza, J. Biener, H. F. Robey, E. L. Dewald, R. Tommasini, L. Divol, and S. Le Pape, L. B. Hopkins, P. M. Celliers, O. Landen, N. B. Meezan, and A. J. Mackinnon, Phys. Rev. E **91**, 021101(R) (2015).
[12] N. Ozaki, K. A. Tanaka, T. Ono, K. Shigemori, M. Nakai, H. Azechi, T. Yamanaka, K. Wakabayashi, M. Yoshida, H. Nagao, and K. Kondo, Phys. Plasmas **11**, 1600 (2004).
[13] P. M. Celliers, D. K. Bradley, G. W. Collins, D. G. Hicks, T. R. Boehly, and W. J. Armstrong, Rev. Sci. Instrum. **75**, 4916 (2004).
[14] See Supplemental Material at http://link.aps.org/supplemental/10.1103/PhysRevLett.125.185701 for details concerning evaluation of uncertainties and plastic deformation stiffness, and the summarized shock data, which includes Refs. [15–17].
[15] A. M. Zaitsev, *Optical Properties of Diamond: A Data Handbook* (Springer-Verlag, Berlin, Heidelberg, 2001).
[16] K. Tanigaki, H. Ogi, H. Sumiya, K. Kusakabe, N. Nakamura, M. Hirao, and H. Ledbetter, Nat. Commun. **4**, 2343 (2013).
[17] J. Eggert, S. Brygoo, P. Loubeyre, R. S. McWilliams, P. M. Celliers, D. G. Hicks, T. R. Boehly, R. Jeanloz, and G. W. Collins, Phys. Rev. Lett. **100**, 124503 (2008).
[18] Y.-Y. Chang, S. D. Jacobsen, M. Kimura, T. Irifune, and I. Ohno, Phys. Earth Planet. Inter. **228**, 47 (2014).
[19] Y. B. Zel'dovich and Y. P. Raizer, *Physics of Shock Waves and High-Temperature Hydrodynamic Phenomena* (Academic Press, New York, 1966).
[20] M. P. Dejarlais and M. D. Knudson, J. Appl. Phys. **122**, 035903 (2017).
[21] M. D. Knudson and M. P. Desjarlais, Phys. Rev. B **88**, 184107 (2013).
[22] C. A. McCoy, Ph. D. thesis, University of Rochester, 2016.
[23] R. S. McWilliams, J. H. Eggert, D. G. Hicks, D. K. Bradley, P. M. Celliers, D. K. Spaulding, T. R. Boehly, G. W. Collins, and R. Jeanloz, Phys. Rev. B **81**, 014111 (2010).
[24] M. D. Knudson, M. P. Desjarlais, and D. H. Dolan, Science **322**, 1822 (2008).
[25] K. Kondo and T. J. Ahrens, Geophys. Res. Lett. **10**, 281 (1983).
[26] M. N. Pavlovskii, Sov. Phys. Solid State **13**, 741 (1971).
[27] M. C. Gregor, D. E. Fratanduono, C. A. McCoy, D. N. Polsin, A. Sorce, J. R. Rygg, G. W. Collins, T. Braun, P. M. Celliers, J. H. Eggert, D. D. Meyerhofer, and T. R. Boehly, Phys. Rev. B **95**, 144114 (2017).
[28] D. G. Hicks, T. R. Boehly, P. M. Celliers, D. K. Bradley, J. H. Eggert, R. S. McWilliams, R. Jeanloz, and G. W. Collins, Phys. Rev. B **78**, 174102 (2008).
[29] M. Millot *et al.*, Phys. Rev. B **97**, 144108 (2018).
[30] X. Zhou, J. Li, W. J. Nellis, X. Wang, J. Li, H. He, and Q. Wu, J. Appl. Phys. **109**, 083536 (2011).
[31] J. M. Lang, J. M. Winey, and Y. M. Gupta, Phys. Rev. B **97**, 104106 (2018).
[32] J. M. Winey, M. D. Knudson, and Y. M. Gupta, Phys. Rev. B **101**, 184105 (2020).
[33] V. V. Zhakhovsky, M. M. Budzevich, N. A. Inogamov, I. I. Oleynik, and C. T. White, Phys. Rev. Lett. **107**, 135502 (2011).
[34] M. J. MacDonald, E. E. McBride, E. Galtier, M. Gauthier, E. Granados, D. Kraus, A. Krygier, A. L. Levitan, A. J. MacKinnon, I. Nam, W. Schumaker, P. Sun, T. B. van Driel, J. Vorberger, Z. Xing, R. P. Drake, S. H. Glenzar, and L. B. Fletcher, Appl. Phys. Lett. **116**, 234104 (2020).
[35] L. X. Benedict, K. P. Driver, S. Hamel, B. Militzer, T. Qi, A. A. Correa, A. Saul, and E. Schwegler, Phys. Rev. B **89**, 224109 (2014).